Article

Removal of Patent Blue (V) Dye Using Indian Bael Shell Biochar: Characterization, Application and Kinetic Studies

Kangkan Roy [1,†], **Kapil Mohan Verma** [1,†], **Kumar Vikrant** [2,†] , **Mandavi Goswami** [1,†],
Ravi Kumar Sonwani [1], **Birendra Nath Rai** [1], **Kowsalya Vellingiri** [3], **Ki-Hyun Kim** [2,*] ,
Balendu Shekher Giri [1,*] **and Ram Sharan Singh** [1]

1   Department of Chemical Engineering and Technology, Centre of Advanced Study, Indian Institute of
     Technology, Banaras Hindu University, Varanasi 221005, India; kangkan.roy.che15@iitbhu.ac.in (K.R.);
     kapilm.verma.che15@itbhu.ac.in (K.M.V.); mandavigs@gmail.com (M.G.);
     raviks.rs.che16@itbhu.ac.in (R.K.S.); bnrai.che@itbhu.ac.in (B.N.R.); rssingh.che@itbhu.ac.in (R.S.S.)
2   Department of Civil and Environmental Engineering, Hanyang University, 222 Wangsimni-Ro, Seoul 04763,
     Korea; kumar.vikrant.che14@itbhu.ac.in
3   Environmental and Water Resources Engineering Division, Department of Civil Engineering, Indian
     Institute of Technology Madras, Chennai 600036, India; kowsalya412@gmail.com
*   Correspondence: kkim61@hanyang.ac.kr (K.-H.K.); bsgiri011@gmail.com or
     balendushekher23@gmail.com (B.S.G.)
†   These authors have contributed equally.

Abstract: The prospective utilization of bael shell (*Aegle marmelos*) as an agro-waste for the production of biochar was investigated along with its characterization and application for the abatement of hazardous aqueous Patent Blue (PB) dye solution. The sorptive removal of PB on bael shell biochar (BSB) was investigated under the following operational conditions: (pH, 2.7–10.4; biochar dosage, 2–12 g/L; and contact time, 0–60 min). The removal efficiency of PB by BSB in a batch adsorption experiment was 74% (pH 2.7 and 30 $\pm$ 5 °C). In addition, a clear relationship between the adsorption and pH of the solution was noticed and the proposed material recorded a maximum sorption capacity of 3.7 mg/g at a pH of 2.7. The adsorption of PB onto BSB was best explained by the pseudo-second order kinetic model (R^2 = 0.972), thereby asserting the predominant role of chemisorption. The active role of multiple surface-active functionalities present on BSB during PB sorption was elucidated with the help of Freundlich isotherm (R^2 = 0.968). Further, an adsorption mechanism was proposed by utilizing Fourier transform infrared spectroscopy (FTIR).

Keywords: adsorption; biochar; dye; kinetics; pollution control; wastewater treatment

1. Introduction

Indian bael (*Aegle marmelos*) is a readily available common fruit widely accessible throughout the regions of India and mostly concentrated in the eastern Gangetic belt region [1]. Usually, the inner portion of the bael fruit is edible. In contrast, the outer part is hard and considered as agro waste. Bael fruit has several medicinal uses in diseases such as piles, edema, jaundice, obesity, pediatric disorders, gastrointestinal diseases, vomiting, gynecological disorders, urinary complaints and as a rejuvenate [2]. Upon the consumption of fruit, the bael shell (BS) is discarded as a waste product. Hence, in this research, the bael shell has been effectively utilized as a biomass feed for synthesizing bio-char and the physicochemical properties of the resulting bio-char are evaluated and analyzed. It is found that bael

shell contains a large number of micro-porous sites, making it a prospective sorbent for the abatement of aqueous contaminants [3].

Dyes are extensively utilized in textile-based industries all over the world as coloring agents [4,5]. Dyes also act as a main pollutant of water in textile industries and the direct disposal of this wastewater into rivers and seas can have a harmful effect on aquatic life and water bodies [4]. Synthetic dyes are the primary constituents of paper, textile, food, cosmetics and pharmaceutical industries due to their large-scale synthesis, stability and color range as compared to naturally produced dyes [6]. Several dyes are known to be extremely hazardous towards human health and ecosystems owing to their high toxicity and carcinogenic tendency [7]. Among many synthetic dyes, patent blue (PB) is widely used as a coloring agent in textile industries. PB dye can cause adverse effects to the human body, including the skin, mucous membranes, eye irritation and allergic diseases [8]. PB can act as an anionic dye to form an ion pair with cationic surfactants in chloroform. Here, cationic surfactants are generally utilized in textile facilities as antistatic and softening agent for textile fiber [9]. The removal of spent PB was difficult due to its enhanced resistance to conventional physicochemical and biological treatment methods.

Several methods are conventionally used in water treatment facilities for the treatment of wastewater containing the excess level of dyes, including oxidation (photochemical and electrochemical) [10,11], Fenton's process [12], membrane separation [13], ion-exchange [14], coagulation [15] and biodegradation [16]. These methodologies are nonetheless found to suffer from several shortcomings such as generation of sludge, applicability to a narrow range of dyes, production of toxic intermediates and low cost-efficiency [17,18]. Among these technologies, the adsorptive removal of dyes has attracted widespread attention owing to its environmental benignity, great selectivity, easy operation and cost-effectiveness [19–21]. At present, pristine and carbonaceous adsorbents are extracted from various agricultural/biological wastes such as coconut shell [22], rice husk [23], rice straws [24], almond shell [25] and wood char [26] for the abatement applications. In this regard, biochar (highly carbonaceous material synthesized through biomass pyrolysis under low oxygen atmosphere) has attracted widespread attention for the sorptive removal of dyes owing to their highly porous structure with great specific surface, cost effective synthesis owing the abundance of waste biomass and highly flexible applicability [27,28].

In this work, batch experiments were performed by utilizing BSB to adsorb PB (V) dye from the aqueous medium. The sorption performance of BSB was evaluated under various situations. To the best of our knowledge, there are limited studies on the use of BSB for the removal of PB dye. Moreover, none of the previous studies explicitly focus on the mechanisms of PB removal by BSB. In light of this limitation, here we have investigated the performance of BSB for PB removal across varying experimental conditions. The obtained results were also fitted in isotherm and kinetic models. Finally, the sorption mechanism was derived with the help of characterization analysis.

2. Materials and Methods

2.1. Chemicals and Adsorbate

PB [(C.I. = 42045, molecular formula = $C_{27}H_{31}N_2NaO_6S_2$, IUPAC Name = (Diethylamino) phenyl] [2,4-disulfophenyl) methylene]-2,5-cyclohexadien-1-ylidene]-N-ethyl-ethanaminium] inner salt sodium salt, λ_{max} = 635 nm, analytical grade, 99% pure) was procured from Sigma-Aldrich, New Delhi, India. The solubility of dye in water was 0.05 gm/L at 20 °C. A 1000 ppm stock solution was made initially. The stock solution was diluted appropriately to produce PB (V) dye solutions of desired concentrations.

2.2. Preparation of Bael Shell Biochar (BSB)

The preparation of biochar was done similarly to the method already reported in the literature [29]. When any biomass is heated above 270 °C, decomposition processes called as carbonization are

initiated. In the absence of oxygen, charcoal is produced as the final product. At about 270 °C, it begins to spontaneously decompose while the heat is evolved simultaneously. Pyrolysis oil also called bio-oil can be obtained by heating dried biomass without oxygen in a reactor at a temperature of about 500 °C with subsequent cooling [29].

First, 10 kg of bael shell was collected from a local juice vendor shop. It was cleaned with deionized water and parched under sunlight for ten days. The dehydrated bael shell was crushed, ground and sieved to a mesh particle size of 60 BSS (250 μm). The bael shell sample was then carbonized at 500 °C for a residence time of 3 h in a Pyrolyzer. The carbonized bael shell sample was cleaned with hot deionized water, dried at 75 °C for 2 h in an oven (Oven Universal NSW-143, New Delhi, India) and then used for further studies.

2.3. Characterization of Bael Shell Biochar (BSB)

2.3.1. Elemental Analysis

Scanning electron microscope (SEM) examination was conducted using a JEOL JSM-6400 Scanning Microscope (JEOL, Tokyo, Japan) at The IIT BHU, Varanasi, India. Various magnifications were used to compare changes or modifications in the structural and surface characteristics of the biochar samples during treatment of Patent Blue dye.

Elemental analyses of bael shell (BS) and bael shell biochar (BSB) were performed to compare the carbon, nitrogen and hydrogen content in BS and BSB using an elemental analyzer, various instruments and software from Euro Vector, Germany. Furthermore, the moisture, ash and volatile matter contents were analyzed for both BS and BSB at different temperature ranges (110, 715 and 930 °C).

The presence of diverse functionalities on BSB surface (before and after sorption process) was examined using FTIR spectroscopy. The spectral range fixed for FTIR analysis was in the range of 4000–400 cm^{-1} using a Thermo-Fisher FTIR analyzer (Nicolet 5700, Tokyo, Japan). Surface morphology of the adsorbent was characterized using an EVO 18 Research Scanning Electron Microscope (SEM), Carl Zeiss, Jena, Germany.

2.3.2. Determination of the Point of Zero Charge of Bael Shell Biochar (BSB)

Point of zero charge (pH$_z$) is a theory developed to account for the sorption mechanism; it specifies the condition at which the surface charge density of the sorbent reaches zero [19,20]. It is generally evaluated in relation to the pH of an electrolyte so that the pH$_z$ value is allocated to a particular colloidal particle or substrate [18]. In this study, the salt addition method was effectively utilized to determine the point of zero charge (pH$_z$). A 0.1M KNO$_3$ solution was made with the initial pH between 2.55–11.3 using 0.1 M solutions of NaOH and HNO$_3$. Later, the pH values were measured using a pH tutor from Eutech Instruments, Singapore. Then, 50 mL of 0.1 M KNO$_3$ was placed in a 150 mL flask and 1g of BSB was added to each flask. An incubation period of 24 h was followed by the subsequent measurement of final pH. A graph was plotted between the initial-final pH difference and the initial pH. The point where ΔpH equals zero was denoted as pH$_z$.

2.4. Batch Adsorption Studies

The batch sorption experiments were conducted by placing 100 mL of PB(V) dye solution of predetermined concentration (50 mg/L) in five different (250 mL capacity) flasks with five different loading amounts of the BSB (0.5, 1.0, 1.5, 2.0 and 3.0 g). The mixture was placed in an incubator shaker (Caltan made orbital shaking incubator cum B.O.D., India) at 110 rpm until equilibrium was observed to be attained. Then, a double beam spectrophotometer (Elico SL 169 operating at λ_{max} = 635 nm) was used to determine the supernatant PB concentration. The sorption percentage of PB (V) dye and equilibrium sorption capacity, q_e (mg/g), was evaluated by:

$$\text{Adsorption } (\%) = \frac{(\text{Ci} - \text{Ce})}{\text{Ci}} \times 100 \tag{1}$$

$$q_e = \frac{(Co - Ce)}{W} \times V \tag{2}$$

where, C_i and C_e are the initial and equilibrium concentrations of PB (V) (mg/L), respectively, *V* is the volume of the dye solution (L) and W is the weight of BSB (g).

2.5. Adsorption Isotherms

In the present study, two isotherms (Langmuir and Freundlich models) were applied to understand the sorption equilibrium. The analysis was conducted by placing 100mL of 50 mg/LPB dye in 250 mL flasks with five different adsorbent dosages as aforementioned. A spectrophotometer was utilized to measure the equilibrium absorbance of the solution. The adsorption capacity and equilibrium solution concentrations were then measured and the suitability of the isotherm was investigated.

2.5.1. Langmuir Isotherm

The Langmuir isotherm model presumes that the sorption processes occur in a monolayer manner. It also assumes that the energy of adsorption is uniform throughout the adsorbed layer on the adsorbent surface, at a constant temperature [30,31].

The linear form of the Langmuir equation can be given as:

$$\frac{C_e}{q_e} = \frac{1}{q_e K_l} + \frac{C_e}{q_m} \tag{3}$$

where q_e (mg/g) is the amount of dye adsorbed at equilibrium, q_m (mg/g) is the amount of dye adsorbed when saturation is attained, C_e is the equilibrium dye concentration (mg/L) and K_l is the Langmuir constant related to the binding strength of the dye onto the adsorbent.

2.5.2. Freundlich Isotherm

The Freundlich isotherm model empirically relates the distribution of solute molecules between the aqueous and solid phases at equilibrium. This isotherm presumes an exponential disparity in the energy of surface-active sorption sites, while the decrease in heat of adsorption is logarithmic [32]. The linearized form of the Freundlich equation is expressed as:

$$\log q_e = \log K_f + \frac{1}{n} \log C_e \tag{4}$$

where, K_f and n are the Freundlich constants that represent adsorption capacity and intensity (strength) of adsorption, respectively. The value of n describes the process as follows: (1) n = 1, a linear process; (2) n < 1, a chemical process; and (3) n > 1, a physical process [33].

2.6. Adsorption Kinetics

To analyze the uptake of PB dye by BSB during sorption, pseudo-first and second order kinetics was applied in this study.

2.6.1. Pseudo-First-Order Kinetic Model

The linear form of the pseudo-first-order kinetic model is represented by

$$\ln(q_e - q_t) = \ln q_e - k_1 t \tag{5}$$

where, q_e and q_t are the values of amount of dye adsorbed per unit mass of adsorbent added at equilibrium and at time t, respectively. In addition, k_1 is the pseudo-first-order adsorption rate

constant (min^{-1}). The values of k_1 and calculated q_e can be determined from the slope and intercept of the linear plot of ln ($q_e - q_t$) versus *t*, respectively.

2.6.2. Pseudo-Second-Order Kinetic Model

The pseudo-second-order kinetic model can be expressed by Equation (6) below,

$$\frac{t}{q_t} = \frac{1}{k_2 q_e^2} + \frac{t}{q_e} \tag{6}$$

where k_2 is the pseudo-second-order adsorption rate constant (g/mg.min) and q_e is the amount of dye adsorbed (mg/g) on the adsorbent at equilibrium. The plot of t/q_t versus t gives a linear relationship, which allows the calculation of k_2 and q_e. Here, it should be noted that the model with a higher regression coefficient (R^2) and agreement between the experimental and calculated value of q_e is utilized as the appropriate model for supporting the adsorption kinetics [34].

3. Results and Discussion

3.1. Characterization

The carbon content of BSB was observed to be highly elevated as compared to the raw biomass through constitutional analysis which can be ascribed to the high carbonization temperature (500 °C) (Table 1). The decrease in nitrogen content of the BSB relative to raw BS is ascribable to the loss of nitrogen-containing functional groups, such as amides or amines that may decompose above 400 °C [35]. The reduced hydrogen content may be due to the eviction of hydrogen as water during pyrolysis.

Table 1. Preparation, proximate, ultimate and elemental analysis of bael shell (BS) and bael shell biochar (BSB).

Methods	Description	Result (%)
Pyrolysis (weight composition)	BSB	29.1
	Bio-oil	22.5
	Gas	49.5
Proximate analysis (Bael Shell)	Moisture (110 °C)	9.20
	Ash (715 °C)	25.7
	Volatile (930 °C)	51.9
Proximate analysis (BSB)	Moisture (110 °C)	4.50
	Ash (715 °C)	310
	Volatile (930 °C)	30.0
Ultimate analysis (Bael Shell)	Carbon	46.2
	Hydrogen	7.46
	Nitrogen	0.56
Ultimate analysis (BSB)	Carbon	72.2
	Hydrogen	2.93
	Nitrogen	0.40

3.2. Point of Zero Charge

The functional groups present in BSB have a significant influence on the point of zero charge of BSB (pH_z). From Figure 1, the ΔpH_z for BSB is 8.80. Here, it is noteworthy to mention that cationic contaminants can be adsorbed on BSB when $pH > pH_z$, while anionic compounds can be adsorbed at $pH < pH_z$. The specific adsorption of cations would shift the value of pH_z lower; whereas, for that of anions, the value of pH_z would shift higher.
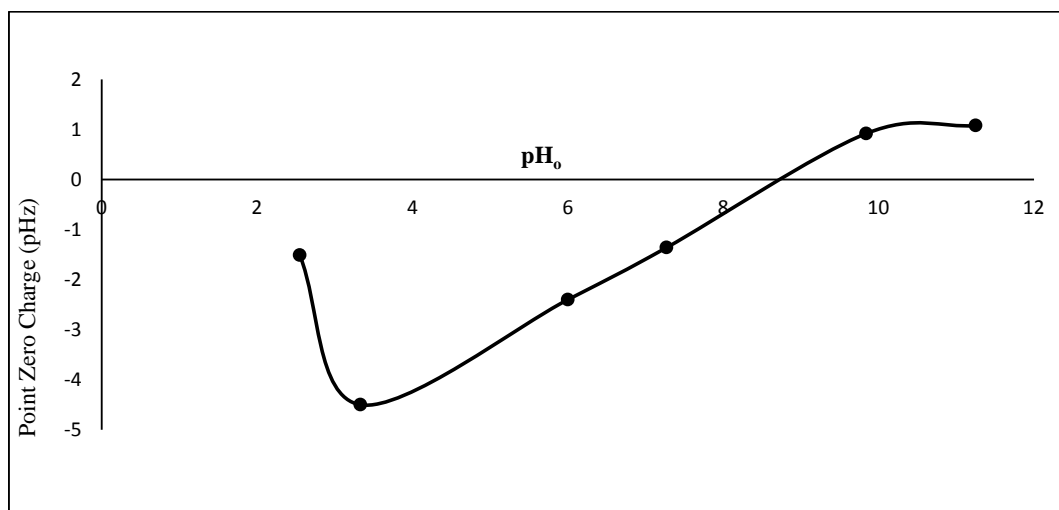
Figure 1. Profile of point of zero charge (ΔpH_z) for adsorbent BSB in adsorption of anionic and cationic dye components.

3.3. Effect of pH on Adsorption of Patent Blue (V)

The initial pH of the solution is a key to determine the extent of PB (V) dye adsorption on the BSB surface. In this respect, when the adsorption of PB was studied in the pH range of 2.7–10.4, maximum sorption was perceived at pH 2.7. The percentage adsorption values of PB onto BSB measured at seven pH points (2.7, 4, 6, 7, 8, 9.2 and 10.4) were 74%, 62%, 58%, 55%, 47%, 40% and 39%, respectively. At lower pH values, the surface charge density of BSB is predominantly positive; thus, adsorbing high quantities of anionic PB dye molecules [36]. The maximum adsorption capacity of BSB towards PB (V) was found to be 3.7 mg/g at a pH of 2.7. Similar adsorption trends were observed for the sorption of PB (V) on Ginger waste material by [8]. These authors obtained a maximum adsorption capacity of 9.56 mg/gat pH 2 with an initial waste concentration of 10 mg/L. The decrease in PB (V) removal upon an increase in pH might be due to competitive adsorption between the hydroxyl ions (OH-) present in the solution and the anionic portions of the PB (V) dye. On the other hand, interference by OH-ions was limited at lower pH values, thus facilitating the attraction of PB anions on a positively charged BSB surface [34,37].

3.4. Kinetic Studies

The reaction pathways and dye removal rate from water can be better understood by adsorption kinetics. The pseudo-first and second order kinetic plots are given in Figure 2. In addition, the corresponding rate constants and regression coefficients (k_1, k_2, q_e and R^2) are outlined in Table 2. The obtained experimental q_e value (2.35 mg/g) was near the calculated q_e of the pseudo-second order kinetic model (2.49 mg/g). Moreover, the resulting regression coefficient value of pseudo-second-order kinetics was higher than the pseudo-first-order kinetics (Table 2). The observed results indicate the sorption process is primarily governed by the pseudo-second-order kinetics. As such, this observation indicates the chemical interaction between BSB and PB (V) dye. Interestingly, activated carbon produced from bael shell has been observed to follow pseudo-second order kinetic model for the sorptive removal of anionic pollutants [38–40].
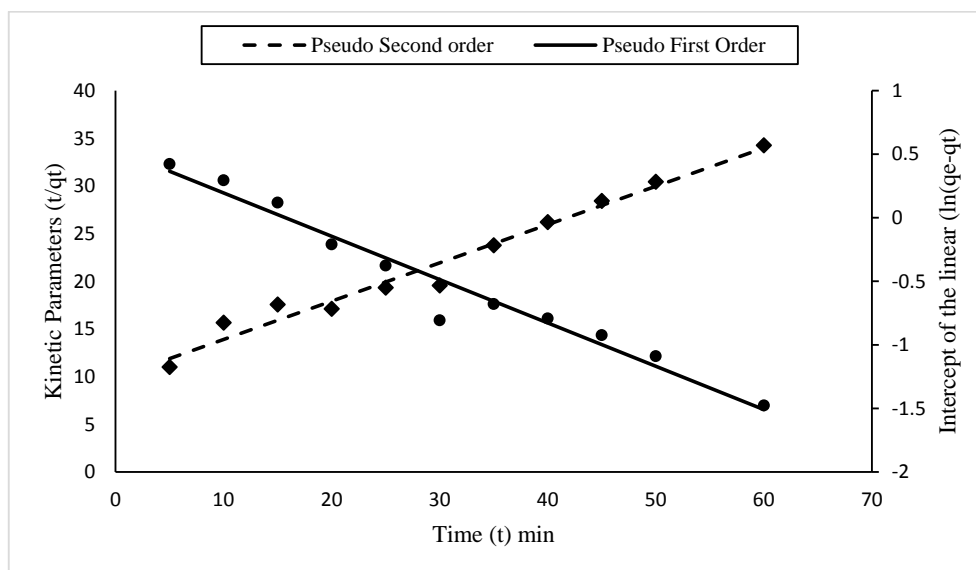
Figure 2. Profile of the pseudo-first- and -second-order kinetics of BSB during the sorption of PB (V) dye.

Table 2. Summary of data obtained for various kinetic and isotherm models of PB (V) dye on BSB.

Reaction Models	Parameters	Values
Pseudo-first-order model	k_1 (L/min)	0.0342
	q_e (mg/g)	1.7225
	R^2	0.9585
Pseudo-second-order model	k_2 (g/mg min)	0.0163
	q_e (mg/g)	2.49
	R^2	0.9723
Langmuir isotherm model	q (mg/g)	16.53
	b (L/mg)	0.00834
	R^2	0.4224
Freundlich isotherm model	KF (mg/g)	0.183
	1/n	0.8264
	R^2	0.968

3.5. Adsorption Isotherm

Freundlich and Langmuir isotherms were applied to reveal the interactions between the equilibrium concentration of PB in solution and the quantity of PB sorbed per unit mass of BSB. The Freundlich and Langmuir isotherm plots are elucidated in Figure 3. The results of the adsorption study are tabulated in Tables 2 and 3. In addition, the value of 1/n is used to indicate the strength of process heterogeneity [41]. For instance, if the value of 1/n is less than 1, it implies the normal Langmuir isotherm models [27]. In contrast, the value of 1/n is above 1, it is indicative of cooperative adsorption. When the value of 1/n becomes close to zero, it may indicate a more heterogeneous process [41]. The isotherm data of PB adsorption on BSB fit well with the Freundlich isotherm model. From the obtained R^2 value of Langmuir (0.4224) and Freundlich isotherm (0.968) models, it was concluded that the latter offered the best fit. In addition, the 1/n value was found to be 0.8264, which indicates a favorable multi-layer adsorption of PB (V) dye onto the positively charged BSB surface. Similar experimental findings were also reported for the sorptive removal of PB via Ginger waste material [8].
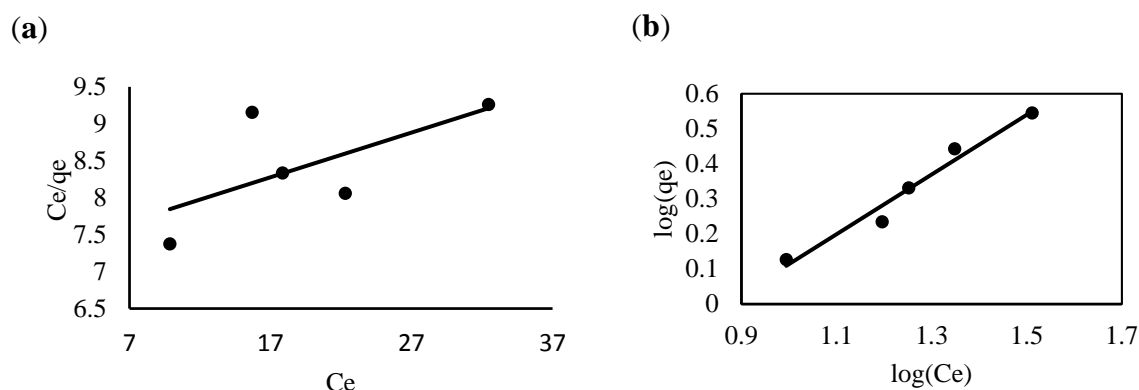
(a)　　　　　　　　　　　　　　　　　　　　　　**(b)**

Figure 3. Summary of different adsorption isotherms for the sorption of PB dye on BSB: (**a**) Langmuir (C_e: Concentration of adsorbate; q_e: Equilibrium dye concentration) and (**b**) Freundlich adsorption isotherm plots.

Table 3. Comparative studies of Patent Blue adsorption on different biochar materials.

Biochar Material	Dye Conc. (mg/L)	Dye Removal	Reference
Paper and pulp sludge	25–100	84.8–90%	[42]
Bottom ash	25–125	4.93–24.3 mg/g	[43]
Korean cabbage	50–5000	1304 mg/g	[29]
Rice straw	50–5000	620.3 mg/g	[29]
Wood chip	50–5000	195.6 mg/g	[29]
Activated carbon	50–5000	271 mg/g	[29]
Hornbeam sawdust	50–500	71%	[44]
Rice husk	50–300	25.8–98.2 mg/g	[45]
Bael shell	50–500	74%	Present Study

3.6. Proposed Mechanism for Adsorption of Patent Blue PB (V) Dye on to Bael Shell Biochar (BSB) Surface

The adsorption of PB dye over the BSB surface can be explained by hydrogen bonding, electrostatic interactions and Vander Waal forces. These interrelationships play a pivotal role in the sorption process, which can be explained in the following points:(a) the carboxylic group present on the BSB surface is expected to completely dissociate at higher pH (basic medium); dissociation would create an ionic repulsion amongst the carboxylate ion of BSB and the negatively charged portion of PB dye molecule, resulting in the reduction of PB dye removal from wastewater compared to lower pH values; (b) the formation of hydrogen bonds between oxygen and nitrogen bearing functionalities of BSB and PB (V) dye; and (c) the Vander Waal forces of attraction can play a role due to the presence of hydrophobic BSB regions and a hydrophilic portion of the PB (V) dye and (d) protonation of carboxylic and hydroxyl groups at lower pH range (acidic medium). In general, carboxylic groups have a pK_a value in the range of 3–5 [36]. At pH < pK_a, carboxylic groups are positively charged and provide a platform for electrostatic attraction via the SO_3-functionalities of PB molecules. On the contrary, the BSB provides a positively charged surface for electrostatic interrelationships with the SO_3-functionality of the PB dye when pH < pH$_z$.

This synergetic effect by BSB for the sorption of PB (V) dye was supported by FTIR analysis. Here, the BSB sample was investigated before and after adsorption at pH 2.3. The peak at 3408.7 cm^{-1} (Figure 4a,b) indicates the presence of H-bonded O–H stretching vibrations of hydroxyl groups from organic acids, alcohols and phenols in BSB, which diminishes after adsorption with PB (V) dye. This decrease in BSB intensity confirms the hydrogen bond formation between PB dye amine and BSB hydroxyl groups. Protonation of hydroxyl and carboxylic groups occurred at lower pH (2.34), which resulted in the ionic interrelationship amongst the anionic PB dye and protonated groups. Furthermore, the shift in BSB peak value from 2523.7 cm^{-1} (Figure 4b) to 2463.9 cm^{-1} (Figure 4b) after adsorption

signifies the interaction of an O–H bond of the carboxylic acid group with dye. The emergence of a new peak at 2889.5 cm^{-1} (Figure 4b) indicates the formation of new –CH stretching vibrations. Moreover, after adsorption, the peak at 1308.1 cm^{-1} belonging to the –SO$_3^{3-}$ functionality was widened and reinforced (Figure 4) for BSB. This clearly indicates that the –SO$_3^-$ group acts as a main functional group for PB dye interaction on the BSB surface (Figure 4). A proposed adsorption pathway of PB (V) dye on to the BSB is given in Figure 5.
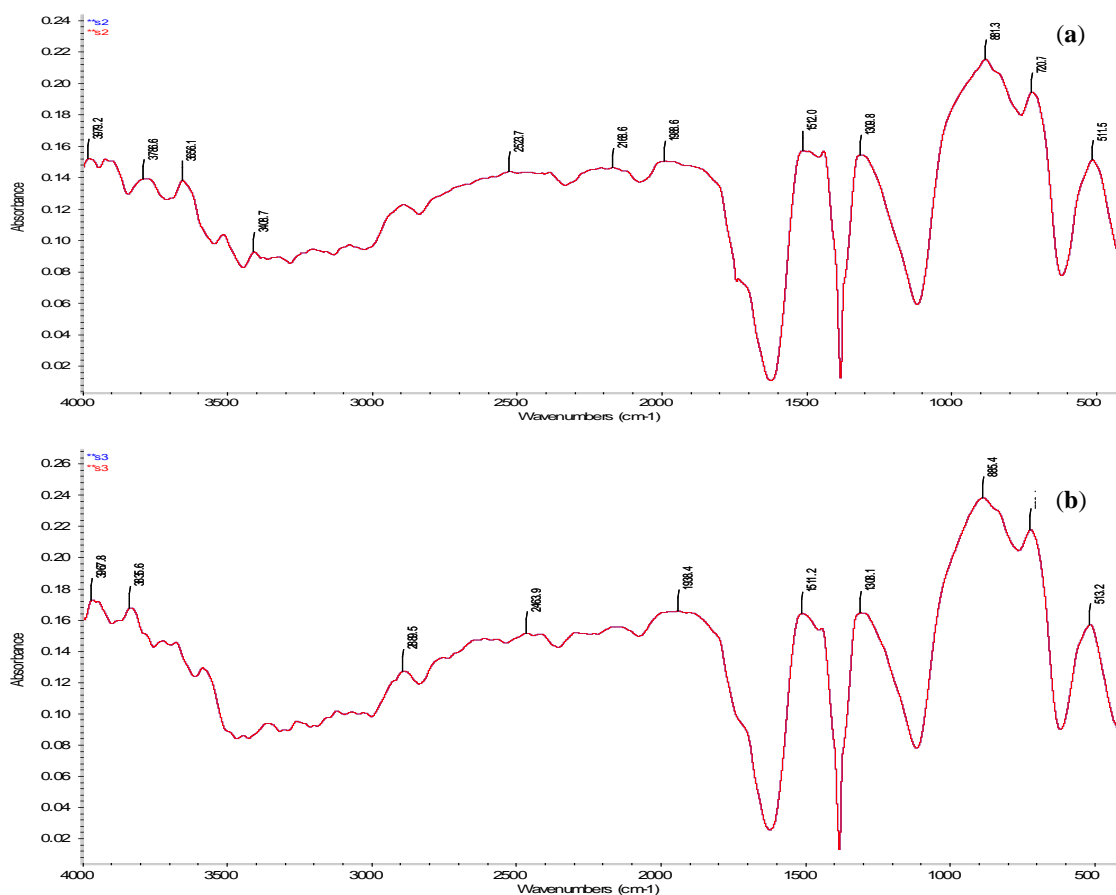

Figure 4. FTIR spectra of Bael Shell Biochar: (**a**) before adsorption of Patent Blue dye at pH 2.32 and (**b**) after adsorption of Patent Blue dye at pH 2.32.
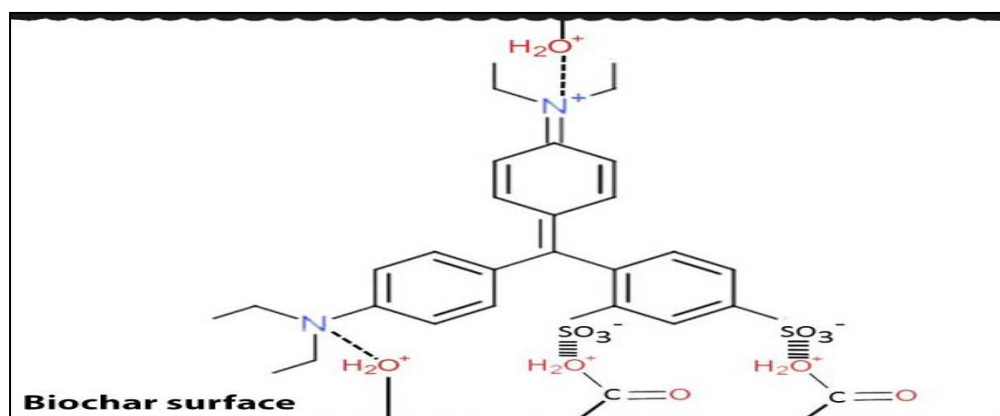

Figure 5. Mechanism of Patent Blue (VI) dye adsorption on to Bael shell biochar (BSB).

3.7. Bael Shell Biochar (BSB) as a Low-Cost Adsorbent for Pollutant Treatment

Biochar can be produced from non-usable materials by thermal conversion in sealed containers, which are rich in carbon content and soil nutrients [27]. In this way, one can reduce waste production in developing regions [46]. This kind of process might reduce the operation cost of conventional sewage-treatment infrastructure. Biochar can also be used for the creation of microporous spaces in which lactic-acid bacteria can inoculate and degrade waste matter at a lower pH value. This kind of degraded material can be used as food for earthworms (Vermiculture) [47]. In this respect, compost can be generated; further treatment of this composite, in the presence of air, over three to 12 months using a Terra preta sanitation process can lead to natural fertilizer [47], which can be sold or used as a fertilizing material for diverse types of vegetation.

On the other hand, the prepared biochar from waste material can be used as an adsorbent for the treatment of diverse pollutants. For instance, the biochar produced from bael shell was found to be a good packing media in a packed bed adsorbent reactor for the removal of Congo red [36]. In another study, up to 52% of fluoride content was removed from waste water upon 60 min of contact time with an adsorbent dose of 2 g/L of BSB [40]. Likewise, the removal efficiency of BSB towards iron was found to approach 60% [48]. The adsorption capacity of BSB towards Cr (VI) was found to be 17.3 mg/g [38].Hence, it is evident that biochar generated from BS biomass is an efficient material for pollutant remediation, especially in wastewater technologies.

3.8. Life Cycle Assessment (LCA) of Biochar Systems

LCA is a well-known technique that is used to analyze the potential impact of the product on the environment throughout the cycle of its usage. One category of environmental impacts included in the commercial LCA software tools are human health, resource use, eutrophication, acidification and photo-oxidants formation [49].

In this study, the raw material used for the production of biochar was bael shell, which is an agro-waste and commonly available in many parts of the world. In comparison with raw bael shell, carbonized bael shell was used to produce both biochar, which was found to be rich in carbon content and bio-oil with a high calorific value of 20.4 MJ/kg [2].The spent BSB can be directly landfilled, which would act as fertilizer for the growth of plants and crops [47]. Here, the pollutant adsorbed on the BSB may be broken down to simpler components by microbial degradation, which can thus act as nutrients for the growth of plants and crops. Moreover, the presence of higher carbon content in the BSB can help increase soil respiration, as well as fungal and bacterial growth rates [50]. In addition, when BSB was fertilized under the soil for three years, the alkalinity of the BSB would decrease slowly by sequential loss of cations such as K, Na and Ca to the soil. The reduced alkalinity may help enhance the growth of the associated microbial community in the soil [50]. Therefore, from the preparation to decomposition of spent BSB, it was concluded that BSB is an appropriate material for contaminant removal.

4. Conclusions

This study focused on the abatement of PB (V) dye from aqueous solutions through the effective utilization of BSB. Initially, the prepared BSB was characterized to determine its surface morphology, composition and type of functional groups. Later, the characterized BSB was utilized for the adsorption of PB (V) dye, which was observed to greatly depend upon the pH of the aqueous solution. The highest removal of PB (V) dye was observed to take place in the lower pH range (pH 2.7) and approached 74%. The obtained highest sorption capacity was noted to be 3.7 mg/g via a chemisorption methodology. The analysis of sorption isotherm revealed that the sorption capacity of BSB was linearly correlated with the amount of PB (V) dye. In addition, the suitability of Langmuir isotherm demonstrated that the adsorption of PB (V) dye was mainly based on the monolayer formation on the BSB surface. The experimental observations of the present investigation show that the bael shell which remains largely unused by the consumers can be used to efficiently remove pigments and dyes

from water/wastewater. Such innovative usage of indigenously produced waste biomass holds a great potential for sustainable waste management as well as a cost-effective control on pollution processes.

References

1. Rahman, S.; Parvin, R. Therapeutic potential of *Aegle marmelos* (L.)—An overview. *Asian Pac. J. Trop. Dis.* **2014**, *4*, 71–77. [CrossRef]
2. Bardalai, M.; Mahanta, D.K. Characterisation of the pyrolysis oil derived from bael shell (*Aegle marmelos*). *Environ. Eng. Res.* **2016**, *21*, 180–187. [CrossRef]
3. Gottipati, R. *Preparation and Characterization of Microporous Activated Carbon from Biomass and Its Application in the Removal of Chromium (vi) from Aqueous Phase; National Institute of Technology Rourkela: Rourkela, India, 2012.*
4. Vikrant, K.; Giri, B.S.; Raza, N.; Roy, K.; Kim, K.-H.; Rai, B.N.; Singh, R.S. Recent advancements in bioremediation of dye: Current status and challenges. *Bioresour. Technol.* **2018**, *253*, 355–367. [CrossRef] [PubMed]
5. Pham, T.D.; Kobayashi, M.; Adachi, Y. Adsorption characteristics of anionic azo dye onto large α-alumina beads. *Colloid Polym. Sci.* **2015**, *293*, 1877–1886. [CrossRef]
6. Bharti, V.; Shahi, A.; Geed, S.R.; Kureel, M.K.; Rai, B.N.; Kumar, S.; Giri, B.S.; Singh, R.S. Biodegradation of reactive orange 16 by dye in the packed bed bioreactor using seeds of Ashoka and Casuarina as packing media. *Indian J. Biotechnol.* **2017**, *16*, 216–221.
7. Padmanaban, V.C.; Geed, S.R.; Achary, A.; Singh, R.S. Kinetic studies on degradation of reactive red 120 dye in immobilized packed bed reactor by *Bacillus cohnii* rapt1. *Bioresour. Technol.* **2016**, *213*, 39–43. [CrossRef] [PubMed]
8. Ahmad, R.; Kumar, R. Adsorption study of patent blue VF using ginger waste material. *J. Iran. Chem. Res.* **2008**, *1*, 85–94.
9. Idouhar, M.; Tazerouti, A. Spectrophotometric determination of cationic surfactants using patent blue v: Application to the wastewater industry in Algiers. *J. Surfactants Deterg.* **2008**, *11*, 263–267. [CrossRef]
10. Cotillas, S.; Llanos, J.; Cañizares, P.; Clematis, D.; Cerisola, G.; Rodrigo, M.A.; Panizza, M. Removal of Procion Red MX-5B dye from wastewater by conductive-diamond electrochemical oxidation. *Electrochim. Acta* **2018**, *263*, 1–7. [CrossRef]
11. Tarkwa, J.-B.; Oturan, N.; Acayanka, E.; Laminsi, S.; Oturan, M.A. Photo-fenton oxidation of Orange G azo dye: Process optimization and mineralization mechanism. *Environ. Chem. Lett.* **2018**, 1–7. [CrossRef]
12. Farshchi, M.E.; Aghdasinia, H.; Khataee, A. Modeling of heterogeneous fenton process for dye degradation in a fluidized-bed reactor: Kinetics and mass transfer. *J. Clean. Prod.* **2018**, *182*, 644–653. [CrossRef]
13. Thamaraiselvan, C.; Michael, N.; Oren, Y. Selective separation of dyes and brine recovery from textile wastewater by nanofiltration membranes. *Chem. Eng. Technol.* **2017**, *41*, 185–293. [CrossRef]
14. Katheresan, V.; Kansedo, J.; Lau, S.Y. Efficiency of various recent wastewater dye removal methods: A review. *J. Environ. Chem. Eng.* **2018**, *6*, 4676–4697. [CrossRef]
15. Lam, S.-M.; Low, X.-Z.D.; Wong, K.-A.; Sin, J.-C. Sequencing coagulation–photodegradation treatment of malachite green dye and textile wastewater through ZnO micro/nanoflowers. *Chem. Eng. Commun.* **2018**, *205*, 1143–1156. [CrossRef]
16. Xiao, X.; Li, T.-T.; Lu, X.-R.; Feng, X.-L.; Han, X.; Li, W.-W.; Li, Q.; Yu, H.-Q. A simple method for assaying anaerobic biodegradation of dyes. *Bioresour. Technol.* **2018**, *251*, 204–209. [CrossRef] [PubMed]

17. Dao, T.H.; Tran, T.T.; Nguyen, V.R.; Pham, T.N.M.; Vu, C.M.; Pham, T.D. Removal of antibiotic from aqueous solution using synthesized TiO_2 nanoparticles: Characteristics and mechanisms. *Environ. Earth Sci.* **2018**, *77*, 359.

18. Pham, T.D.; Nguyen, H.H.; Nguyen, N.V.; Vu, T.T.; Pham, T.N.M.; Doan, T.H.Y.; Nguyen, M.H.; Ngo, T.M.V. Adsorptive removal of copper by using surfactant modified laterite soil. *J. Chem.* **2017**, *2017*, 1986071. [CrossRef]

19. Pham, T.; Bui, T.; Nguyen, V.; Bui, T.; Tran, T.; Phan, Q.; Pham, T.; Hoang, T. Adsorption of polyelectrolyte onto nanosilica synthesized from rice husk: Characteristics, mechanisms, and application for antibiotic removal. *Polymers* **2018**, *10*, 220. [CrossRef]

20. Pham, T.D.; Do, T.T.; Ha, V.L.; Doan, T.H.Y.; Nguyen, T.A.H.; Mai, T.D.; Kobayashi, M.; Adachi, Y. Adsorptive removal of ammonium ion from aqueous solution using surfactant-modified alumina. *Environ. Chem.* **2017**, *14*, 327–337. [CrossRef]

21. Sophia, A.C.; Lima, E.C. Removal of emerging contaminants from the environment by adsorption. *Ecotoxicol. Environ. Saf.* **2018**, *150*, 1–17. [CrossRef] [PubMed]

22. Bello, O.S.; Ahmad, M.A. Coconut (*Cocos nucifera*) shell based activated carbon for the removal of malachite green dye from aqueous solutions. *Sep. Sci. Technol.* **2012**, *47*, 903–912. [CrossRef]

23. Singh, D.K.; Srivastava, B. Basic Dyes Removal from Wastewater by Adsorption on Rice Husk Carbon. *Indian J. Chem. Technol.* **2001**, *8*, 133–139.

24. El-Sonbati, A.Z.; El-Deen, I.M.; El-Bindary, M.A. Adsorption of hazardous azorhodanine dye from an aqueous solution using rice straw fly ash. *J. Dispers. Sci. Technol.* **2016**, *37*, 715–722. [CrossRef]

25. Doulati Ardejani, F.; Badii, K.; Limaee, N.Y.; Shafaei, S.Z.; Mirhabibi, A.R. Adsorption of direct red 80 dye from aqueous solution onto almond shells: Effect of PH, initial concentration and shell type. *J. Hazard. Mater.* **2008**, *151*, 730–737. [PubMed]

26. Bangash Fazlullah, K.; Manaf, A. Dyes removal from aqueous solution using wood activated charcoal of bombax cieba tree. *J. Chin. Chem. Soc.* **2013**, *52*, 489–494. [CrossRef]

27. Vikrant, K.; Kim, K.-H.; Ok, Y.S.; Tsang, D.C.W.; Tsang, Y.F.; Giri, B.S.; Singh, R.S. Engineered/designer biochar for the removal of phosphate in water and wastewater. *Sci. Total Environ.* **2018**, *616–617*, 1242–1260. [CrossRef] [PubMed]

28. Zazycki, M.A.; Godinho, M.; Perondi, D.; Foletto, E.L.; Collazzo, G.C.; Dotto, G.L. New biochar from pecan nutshells as an alternative adsorbent for removing reactive red 141 from aqueous solutions. *J. Clean. Prod.* **2018**, *171*, 57–65. [CrossRef]

29. Sewu, D.D.; Boakye, P.; Woo, S.H. Highly efficient adsorption of cationic dye by biochar produced with Korean cabbage waste. *Bioresour. Technol.* **2017**, *224*, 206–213. [CrossRef] [PubMed]

30. Al-Ghouti, M.A.; Khraisheh, M.A.M.; Allen, S.J.; Ahmad, M.N. The removal of dyes from textile wastewater: A study of the physical characteristics and adsorption mechanisms of diatomaceous earth. *J. Environ. Manag.* **2003**, *69*, 229–238. [CrossRef]

31. Bharathi, K.S.; Ramesh, S.T. Removal of dyes using agricultural waste as low-cost adsorbents: A review. *Appl. Water Sci.* **2013**, *3*, 773–790.

32. Ng, C.; Losso, J.N.; Marshall, W.E.; Rao, R.M. Freundlich adsorption isotherms of agricultural by-product-based powdered activated carbons in a geosmin–water system. *Bioresour. Technol.* **2002**, *85*, 131–135. [CrossRef]

33. Senthil Kumar, P.; Palaniyappan, M.; Priyadharshini, M.; Vignesh, A.M.; Thanjiappan, A.; Sebastina Anne Fernando, P.; Tanvir Ahmed, R.; Srinath, R. Adsorption of basic dye onto raw and surface-modified agricultural waste. *Environ. Prog. Sustain. Energy* **2013**, *33*, 87–98.

34. Zhou, Y.; Ge, L.; Fan, N.; Xia, M. Adsorption of congo red from aqueous solution onto shrimp shell powder. *Adsorpt. Sci. Technol.* **2018**, *36*, 1310–1330.

35. Vautard, F.; Grappe, H.; Ozcan, S. Stability of carbon fiber surface functionality at elevated temperatures and its influence on interfacial adhesion. *Appl. Surf. Sci.* **2013**, *268*, 61–72. [CrossRef]

36. Ahmad, R.; Kumar, R. Adsorptive removal of congo red dye from aqueous solution using bael shell carbon. *Appl. Surf. Sci.* **2010**, *257*, 1628–1633. [CrossRef]

37. Prasad, A.L.; Santhi, T. Adsorption of hazardous cationic dyes from aqueous solution onto acacia nilotica leaves as an eco friendly adsorbent. *Sustain. Environ. Res.* **2012**, *22*, 113–122.

38. Anandkumar, J.; Mandal, B. Removal of cr(VI) from aqueous solution using bael fruit (*Aegle marmelos correa*) shell as an adsorbent. *J. Hazard. Mater.* **2009**, *168*, 633–640. [CrossRef] [PubMed]

39.　Gottipati, R.; Mishra, S. Process optimization of adsorption of cr(vi) on activated carbons prepared from plant precursors by a two-level full factorial design. *Chem. Eng. J.* **2010**, *160*, 99–107. [CrossRef]

40.　Singh, K.; Lataye, D.H.; Wasewar, K.L. Removal of fluoride from aqueous solution by using bael (*Aegle marmelos*) shell activated carbon: Kinetic, equilibrium and thermodynamic study. *J. Fluor. Chem.* **2017**, *194*, 23–32. [CrossRef]

41.　Hameed, B.H.; Din, A.T.M.; Ahmad, A.L. Adsorption of methylene blue onto bamboo-based activated carbon: Kinetics and equilibrium studies. *J. Hazard. Mater.* **2007**, *141*, 819–825. [CrossRef] [PubMed]

42.　Azizi, A.; Moghaddam, M.R.A.; Arami, A. Removal of a reactive dye using ash of pulp and paper sludge. *J. Residuals Sci. Technol.* **2012**, *9*, 159–168.

43.　Saleh, S.M.; Maarof, H.I.; Rahim, S.N.S.A.; Nasuha, N. Adsorption of Congo Red onto Bottom Ash. *J. Appl. Sci.* **2012**, *12*, 1181–1185. [CrossRef]

44.　Ates, F.; Tezcan Un, U. Production of char from hornbeam sawdust and its performance evaluation in the dye removal. *J. Anal. Appl. Pyrolysis* **2013**, *103*, 159–166. [CrossRef]

45.　Duraisamy, R.; Kiruthiga, P.M.; Hirpaye, B.Y.; Berekute, A.K. Adsorption of azure b dye on rice husk activated carbon: Equilibrium, kinetic and thermodynamic studies. *Int. J. Water Res.* **2015**, *5*, 18–28.

46.　Breulmann, M.; Schulz, E.; van Afferden, M.; Müller, R.A.; Fühner, C. Hydrochars derived from sewage sludge: Effects of pre-treatment with water on char properties, phytotoxicity and chemical structure. *Arch. Agron. Soil Sci.* **2018**, *64*, 860–872. [CrossRef]

47.　Ye, J.; Zhang, R.; Nielsen, S.; Joseph, S.D.; Huang, D.; Thomas, T. A combination of biochar–mineral complexes and compost improves soil bacterial processes, soil quality, and plant properties. *Front. Microbiol.* **2016**, *7*, 372. [CrossRef] [PubMed]

48.　Anusha, G. Removal of iron from waste water using bael fruit shell as adsorbent. In Proceedings of the 2nd International Conference on Environmental Science and Technology (IPCBEE), Singapore, 26–28 February 2011; IACSIT Press: Singapore, 2011; Volume 6, pp. 260–285.

49.　Smebye, A.B.; Sparrevik, M.; Schmidt, H.P.; Cornelissen, G. Life-cycle assessment of biochar production systems in tropical rural areas: Comparing flame curtain kilns to other production methods. *Biomass Bioenergy* **2017**, *101*, 35–43. [CrossRef]

50.　Jones, D.L.; Rousk, J.; Edwards-Jones, G.; DeLuca, T.H.; Murphy, D.V. Biochar-mediated changes in soil quality and plant growth in a three-year field trial. *Soil Biol. Biochem.* **2012**, *45*, 113–124. [CrossRef]